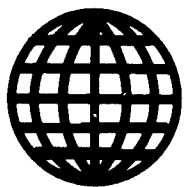JPRS-UEE-92-008
5 AUGUST 1992
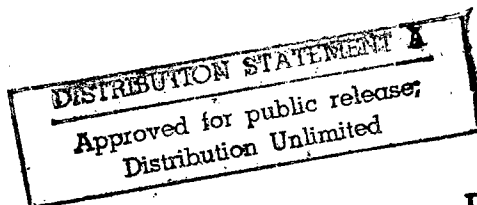
FOREIGN
BROADCAST
INFORMATION
SERVICE

JPRS Report

Science & Technology

Central Eurasia:
Electronics & Electrical Engineering

19980114 182

Science & Technology
Central Eurasia: Electronics & Electrical Engineering

CONTENTS

Power Engineering

Industrial Applications

Basic Power Supply Module BPK-2 for 2-6.5 kW Xenon Lamps

[Article by G.M. Klyushin and M.L., All-Union Scientific Research Institute of Cinematography, V.S. Danilov and A.M. Oleynikov, Samarkand Instrument Design Engineering Office; UDC 621.311.6:778.55]

[Abstract] An electric power supply for series DKsEl 2-6.5 kW xenon lamps has been developed, the power output of the basic BPK-2 module being determined by the peak current and voltage ratings of its high-frequency TB-251-100 thyristors and DCh-251-200 diodes. Its operating scheme involves intermediate inversion of the rectified line voltage into a high-frequency voltage by a resonance inverter with the two thyristors in series for pulse-frequency regulation of the output current. The rectifier is connected to a 3-phase 380 V AC line directly without transformer through an automatic on-off switch, a magnetic starter, and a set of interference suppressor filters. The rectifier output voltage passes through a smoothing filter to the inverter. The high-frequency inverter output voltage proceeds to a high-frequency matching step-down transformer with two secondary windings for two identical low-voltage rectifiers. Each rectifier is followed by a smoothing LC-filter, whereupon both are connected in parallel across the load. The load current is stabilized and regulated through a current sensor, a signal amplifier, an automatic regulator, and a shaper of control signals. The power supply module contains also a trickle feed device which shapes the no-load voltage and a protective device for the power components, both devices and the control devices being energized by a separate transformer-rectifier set across the 380 V AC line. After the power supply has been started, its output voltage builds up to about 120 V needed for breakdown of a lamp by the ignitor in a movie projector. Two capacitors included in the power supply module subsequently discharge through the lamp so as to drive it into a nearly nominal mode, whereupon its transition to a state of glow is triggered. Figures 6; references 2.

Influence of Motion Picture Apparatus on Picture Definition

[Article by M.Ya. Troitskaya, Leningrad Institute of Motion Picture Engineers; UDC 778.5:771.537+778.53(47+57)]

[Abstract] The performance of a four-stage motion picture system consisting of the following components (camera - three printers - projector - viewing room with screen - visual analyzer) and processing four photographic films (negative - high contrast - positive - slide) is evaluated with regard to picture definition, considering all factors contributing to its degradation. In the camera the factors contributing to this degradation are instability of the film position in the frame window during exposure, mechanical vibration, light scattered inside, discrepancy between lens-to-object distance and base distance, and less than optimum focusing of the camera lens. While in intermittent-duty printers the contributing factors are the same as in the camera, in continuous-duty printers the contributing factors are mutual shifting of film tapes on the printer drum, gap between film frames within the printing zone, and finite width of the slot. In the projector the contributing factors are axial instability of the film frame owing to thermal "shock", mechanical vibration, less than optimum focusing of the projector lens, and light scattered over the viewing room. With an information index selected as measure of picture definition, a quantitative analysis involving the space-frequency characteristics of all system components indicates how the picture definition will depend on the type of equipment used in the system. The quality of a picture appearing on the screen has been evaluated in accordance with the following algorithm: 1) calculate the space-frequency characteristic of the system as the product of those of all six system components, 2) refer the space-frequency characteristic to the surface area of the viewer's eye retina so as to account for the viewer's position relative to the screen, 3) calculate the information index as the ratio of information density in the optical signal received by the analyzer (eye) viewing the image to information density in the optical signal received by the analyzer (eye) viewing the object, 4) gauge the picture definition on a point scale against the sensory perception characteristic of the analyzer (eye). Such an evaluation has been made for various "Konvas-Avtomat" cameras and various 23KPK projectors, using three grades of photographic film (LN-8, KP-6, TsP-8R) manufactured in the USSR. The results indicate a large variance of the space-frequency characteristics within each type of motion picture equipment, especially among projectors, and a consequently insufficient parametric reliability of the equipment with respect to picture definition. With those photographic films, however, it may nevertheless be feasible to obtain pictures with excellent definition by using a two-stage printing process. Figures 4; tables 2; references 4.

Scattering of Radio Waves in the Millimeter Range by Laser Induced Discharges in a Dust-Laden Atmosphere

[Article by A. G. Kislyakov, V. A. Kanakov, Yu. M. Sorokin, S. Ye. Finkelshteyn, Nizhegorod State University; UDC 621.371.361]

[Abstract] One of the factors limiting the development of super-wideband stable communication channels in the millimeter and sub-millimeter range is a strong absorption of the radio waves by atmospheric gases. Since the absorption coefficient in gases quickly diminishes with elevation, the efficiency of employing oblique paths with passive scatterers was examined by comparing it with the integral absorption of the mm range radio waves in atmospheric gases when using a near-ground path. It was shown that an oblique path with a reflector was in fact more efficient than a horizontal.

One way of creating artificial scatterers is to stimulate a Collective Optical Discharge (COD) in the atmosphere's aerosol by a powerful laser pulse. The available laser systems can produce such a discharge at elevation of about hundred meters, which would extend the radio horizon range to 40 km.

Feasibility was demonstrated by employing the optical discharge as a repeater for communication lines in the mm range at distances of up to 40 km. Figures 2, references 8: 6 Russian, 2 Western.

Electroacoustic Sounding of the Atmosphere

[Article by S. V. Polyakov, V. O. Rapoport, V. Yu. Trakhtengerts, Scientific Research Radiophysics Institute; UDC 621.371.361]

[Abstract] Electrical parameters of the atmosphere, such as the electric field, density of the space charge, conductivity, etc are important indicators of its condition. With the existing methods for measuring these parameters the instruments located on the ground or on board of an aircraft or a rocket measure the parameters in their vicinity. This method is acceptable for measurements of the near-ground atmosphere, but many difficulties arise with measurements at high elevations or in centers of active disturbances. A new remote measurements method is proposed in this paper which employs scattering of a probing acoustical signal in the active regions of the atmosphere with transformation of the acoustical signal into an electromagnetic signal due to non-compensated space charge. For this method time-space synchronism of the acoustic waves and atmospheric

heterogeneities is significant. Theoretical justifications are provided and the estimates are made of possible effects. References 2 Russian.

Experimental Study of the Adaptive System for Active Suppression of the Wideband Acoustic Field in a Pipeline with Unmatched Ends

[Article by A. A. Belyakov, A.A. Maltsev, S. Yu. Medvedev, V.V. Cherepennikov, Nizhegorod State University; UDC 534.832:62-532.8]

[Abstract] Results are described of an experimental study of an adaptive system for active suppression of the wideband acoustic field in a duct. In the experiment, the duct was made of stainless steel filled with fresh water, and the adaptive system for active suppression consisted of two primary receivers of the original field located along the duct axis, two suppressing radiators, and two control receivers of the residual field. The original field was excited by a radiator located at the end face flange of the duct. A unidirectional reception and generation of the hydroacoustic oscillations was provided by electronic devices. The residual wave power after attenuation served as a measure of the system's efficiency. Graphs were drawn showing normalized spectral power densities of the residual field and the original field with disconnected suppression system. Using this system it was possible to achieve the acoustic field suppression on the order of 20-30dB in the 1100-1700 Hz frequency range and 17dB in the 500-2500 Hz range. Figures 6, references 12: 8 Russian, 4 Western.

Surface Potential Method for the Problem of Wave Diffraction by a Permeable Cylinder With Arbitrary Cross-Section in a Stratified Medium

[Article by A. G. Yarovoy, Kharkov State University; UDC 537.874.4]

[Abstract] A theoretical study was performed for the solution of a two-dimensional diffraction problem by a uniform permeable cylinder with arbitrary cross-section using a numerical approach.

The particular features of the developed algorithm consist in the the use of surface potentials for a single or a double layer with Green functions for space-heterogeneous medium to obtain a Fredholm type system of integral boundary equations (SIBE) of the second kind, along with the application of the mechanical quadrature method for the SIBE quantization.

A system of integral equations was derived and a universal algorithm developed for their solution. Because the fields can be represented as potentials of a single or a double layer, or a linear combination, additional conditions for the surface potential density can be arbitrarily specified. The method of the surface potentials produces a system of integral or integral-differential equations of the second kind. This fact significantly expands the range of the method compared to the Green equations method, and in many cases allows to construct more effective numerical algorithms. Figures 5, references 15: Russian 9, Western 6.

Experimental Study of Non-Reciprocity of the Meteor Radio Channel

[Article by A. Ye. Bazlov, T. V. Kazakova , A. R. Kurganov, R. R. Merzakreyev, V. V. Sidorov, R. G. Khuzyashev, L. A. Epiktetov, Kazan State University; UDC 537.874.6]

[Abstract] A method which assumes a reciprocity of the meteor channel is used for synchronization of the time scale in the meteor radio systems. With instrumental errors of the synchronization systems on the order of 0.1 microseconds, the assumption of reciprocity is valid; however, if the error is reduced down to several nanoseconds, the non-reciprocity of the meteor radio channel is determined experimentally.

In order to determine the non-reciprocity characteristics of the meteor channel, data of experimental observations conducted in September 1988 between Moscow and Leningrad were examined and compared with similar experimental results obtained in 1979.

Noise non-reciprocity at both points is always present. Because of this fact a non-identical average value of the meteor echo amplitudes was recorded at both points for identical signal to noise ratio. A wide dispersion of the amplitude logarithm's ratio in the 0.4-1.4 range indicates the existence of an amplitude non-reciprocity of the meteor channel.

Based on the results of the two experiments the non-reciprocity in the meteor radio channel was reliably established. However, its quantitative estimates and comparison with the results of mathematical modeling require a further study. Because of insufficient statistical data it was not possible to determine if there are any variations in the distribution rate of the phase difference between day time and night time meteor echo. More accurate measurements of the echo-signal amplitude are needed. Figures 1, references 5 Russian.

Transformation of a Single-Pulse Echo into a Two-pulse Echo With Change of the Exitation Pulse Shape

[Article by G. G. Fedoruk, V. I. Tsifrinovich, A. D. Tarasevich, Institute of Physics Siberian Branch of Russian Academy of Sciences; Scientific Research Institute for Applied Physical Problems at Byelorus University; UDC 539.143.43]

[Abstract] Response of the Hahn system to a radio frequency pulse under conditions of non-uniform widening of the magnetic resonance line exhibits some peculiar features depending on the relationship between the parameters of the excitation pulse and the system. Particularly, it occurs when the amplitude of a rectangular radio frequency pulse has an oscillating character and attenuates some times after the pulse cutoff. It was previously demonstrated that if the excitation pulse has protrusions, whose amplitudes are greater than the amplitude of the pulse, a single-pulse echo signal is formed in the system. When the pulse amplitude is decreased, the single-pulse echo gradually transforms into a two-pulse echo. This transformation was examined experimentally and it was verified that the signal qualitative behavior corresponds to the theoretical computations. Figures 3, references 3: 2 Russians, 1 Western.

Experimental Apparatus for Focusing High-Intensity Microwave Radiation Flux in Free Space

[Article by G.I. Batskikh and Yu.I. Khvorostyanoy; UDC 621.396.07]

[Abstract] Industrial applications for microwave radiation are being studied in an experimental facility including an electrophysical apparatus at the Moscow Institute of Radio Engineering, the usefulness of microwave radiation in both scientific study of microwave-discharge plasmas and for practical purposes such as ameliorating treatment of structural materials or in agriculture depending largely on the feasibility of generating a high-intensity electromagnetic microwave radiation fluxes in free space and focusing it on a specific targets. The apparatus is essentially a multi(192)-channel 7 GHz (2.34 cm) transmitter with a symmetric horn-antenna array radiating into a vacuum chamber. Each channel consists of a 100 kW klystron amplifier of signals coming from a common exciter through a distributing waveguide-cable which consists of twin-T bridges. The antenna radiates a power of approximately 20 MW, disregarding losses, with an about 10 MW power concentrated within a focal spot about 5 cm in diameter. A power density of the order of 0.1 MW/cm^2 is attained by cophasing the radiation signals from all channels. By means of special metal-plastic lenses placed in the aperture of each horn, it is possible to change the polarization of the microwave radiation from a vertical linear one to a nearly circular elliptic one. The horizontally disposed cylindrical vacuum chamber is 4 m in diameter and 8 m long, a 11.3 cm thick polyethylene entrance window 2 m in diameter transparent to radio-frequency radiation facing the transmitter antenna array. The parameters of microwave-discharge plasma can be regulated by varying either the radiation power density within the duration of a radiation pulse or by varying both duration and repetition rate of the radiation pulses. The first method is implemented by means of a device which appropriately manipulates the excitation signal fed to the klystrons so that 2-step or 3-step pulses can be formed and the radiation power density in the focal spot thus almost instantaneously changed up to three times within the duration of such a pulse. The second method is implemented by program control with the aid of a CAMAC computer, making it possible to change pulse duration and repetition rate at 250 arbitrary time intervals. The position of the focal spot and the distribution of the electromagnetic field over that spot are also controllable, inasmuch as phase control is effected in each channel independently and the phase distribution over the antenna aperture can thus be varied for any given purpose. Figures 3.

Some Modifications of Microwave Relativistic-Electronic Devices

[Article by A.A. Kurayev, B.M. Paramonov, and A.K. Sinitsyn; UDC 621.378.325]

[Abstract] As a contribution to further improvement and development of microwave relativistic-electron devices, there are described two modifications of free-electron lasers, four modifications of the klystrode (tetrode-klystron), and a pulsed version of the gyrotron. The first modification of the electrostatic free-electron is an electric wiggler replacing the magnetic one, replacement of large heavy magnets with compact much less weighing plates making it possible to decrease the pole pitch and thus raise the operating frequency. While the relativistic electron beam interacts with a partial T_{00n} resonator-mode ($n \gg 1$) companion wave in the open resonator cavity formed by two convex mirrors, successive reflections of its electrons by the electrostatic wiggler mirrors give rise to its transverse modulation within the interaction space. The second modification of the electrostatic laser is a wide tubular of solid cylindrical relativistic electron beam replacing the ribbon beam and interacting with a partial E_{01n} resonator-mode companion wave within the resonant segment of an irised waveguide. Another possible modification of a free-electron laser is replacement of the periodically distributed static fields with a uniform electric field and a uniform magnetic field crossing each other, as they do in a cyclotron-resonance laser, so that a trochoidal relativistic electron beam will be formed. All proposed modifications of the klystrode feature distributed energy extraction. In its first modification (hot cathode - modulating cavity resonator with control grid - accelerating anode - corrugated waveguide - collector) energy of the relativistic electron beam is extracted from the resonant waveguide segment. In its second modification (hot cathode - modulating cavity resonator with control grid - accelerating anode - magnetic wiggler - collector) energy of the relativistic electron beam is extracted from the wiggler. In its third modification (hot cathode - modulating cavity resonator with control grid - accelerating anode - retarding structure with cold cathode - collector) energy of electron bunches is extracted in crossed fields interacting with the retarding field. In its fourth modification (hot cathode - modulating resonator with control grid - pair of permanent magnets producing a transverse magnetic field - open resonator inside solenoid producing a longitudinal magnetic field) electron bunches are first twisted in the transverse magnetic field and their energy is then extracted from the resonator under conditions of gyroresonance. In a pulsed gyrotron the amplification mechanism is analogous to that in the betatron and thus differs from that in the continuous-duty gyrotron, where amplification takes place in a rising or periodic longitudinal magnetic field which slows down the relativistic electron beam by converting the longitudinal drift

velocity of its electrons into a rotational transverse one without changing their total energy. In a pulsed gyrotron the electron gun forms successive short linear relativistic electron beams. Each of them enters the modulating open input resonator, where its transverse oscillations are converted (by an external source) into rotational ones so that it is swept circularly at the input signal frequency around its original axis or around the resonator axis. From here it proceeds through a pump tube into the cavity output resonator, both tube and resonator inside a pulsed solenoid. The solenoid current pulses must be synchronized with the beam current pulses and the magnetic field of the solenoid must continue building up as long as a beam travels through the tube. The magnetic field must then remain constant at its maximum intensity till a beam has passed from the output resonator to the collector, that maximum intensity corresponding to conditions of gyroresonance in the output resonator. Figures 5; references 12 Russian.

Spectroscopy of Photoelectrons With High Angle and Energy Resolution from GaAs Emitter With Negative Electron Affinity

[Article by V.V. Korablev, Yu.A. Kudinov, M.Sh. Sugaipov, and T.D. Baranova; UDC 537.533]

[Abstract] Three variants of the electron emission process in semiconductors are compared with respect to possible angular distributions of electrons at fixed energy levels. Two variants represent extreme situations: 1) absence of scattering, electrons assumed to have been thermalized at Γ-minimum level of the conduction band; 2) complete momentum relaxation in the space charge region, length of the relaxation path assumed to be much smaller than width of the space charge region. As the third variant is considered electron emission from dimensional quantization states (surface subbands). The comparison is based on experimental data, photoelectrons with high angle and energy resolution having been recorded in a dispersive analyzer with a plane of symmetry and with a double permalloy shield keeping out magnetic fields. As emitters with negative electron affinity were used epitaxial GaAs(111):B films with a $p= 5 \times 10^{18} cm^{-3}$ hole concentration, also such films activated with Cs or with oxygen. The data reveal fairly wide energy spectra of photoelectrons (1.1-1.9 eV) leaving such emitters and quite narrow angular distributions (from -30° to +10°) of electrons leaving the emitter with various amounts of kinetic energy from 0.05 eV to 0.4 eV, the widest exit angle depending on and increasing with the excess electron energy above the bottom of the conduction band. Such a narrowness of the angular distribution may be due to focusing of slow electrons by the emitter surface with a nonuniform potential distribution. Figures 5; references 8.

Localized Valence-Band States of Photostimulated Exoelectron Emission by PbO-SiO₂ Glasses

[Article by A.F. Zatsepin, V.S. Kortov, and Yu.V. Shchapova; UDC 539.213:537.533.2]

[Abstract] An experimental study of photostimulated exoelectron emission by glasses of the $PbO-Si_2$ series was made concerning the role of intrinsic localized valence-band states in this process. The composition xPbO x $(1-x)SiO_2$ was varied over the x= 0.3-0.6 range and correspondingly the type short-range order as well as the degree of glass grid disorder, making it possible to thus easily vary the parameters of those valence-band states. The photostimulation channel consisted of an LDS-400 deuterium lamp, a DMR-4 dual monochromator, and an optical entrance window made of quartz glass. The exoelectron emission spectra were recorded under a vacuum of 0.1 mPa, with a VEU-6 secondary-electron multiplier used as exoelectron detector, and the optical absorption spectra of 0.6-0.8 mm thick glass plates were measured with a Specord-40M spectrophotometer. The relative quantum yield was measured with correction for dispersion of the transmission coefficient along the optical channel, its dispersion being estimated by the intensity of glow of sodium salicylate. The dependence of photostimulated exoelectron emission current was found on the quantum energy was found to be exponential, unlike its power-law dependence in the initial low-energy quantum range characteristic of most crystalline materials. Both the optical absorption and the energy gap E_g were found to decrease bilinearly with increasing PbO content, less so over the x= 0.3 to x= 0.45-0.5 range and more so over the x= 0.45-0.5 to x= 0.6 range. The data are consistent with earlier data pertaining to centers induced by radiation and thermally ionized ionization on intrinsic localized states near the bottom of the conduction band. Both the nature and the concentration of intrinsic localized states in the upper part of the valence band thus evidently changes as the PbO content (x) changes. Measurements made over the 230-360 K temperature range reveal that the intensity of photostimulated exoelectron emission increases and the intensity of intrinsic luminescence decreases with rising temperature, while the parameter E_0 in the expression $J(hv,T)= J_0(T)exp[hv/E_0(T)]$ (J - emission current, hv - energy of light quantum, T - absolute temperature) remaining almost constant for glass with x= 0.6 and increasing steeply for glass with x= 0.3 as these glasses are heated from 230 K to room temperature. These trends indicate photostimulated exoelectron emission by these glasses is strongly influenced by the dynamic disorder, the ratio of dynamic to static effects in the exponential broadening of the quantum yield spectrum changing as the short-range order of the Pb sublattice changes and correspondingly the atomic-electronic structure of the glass matrix also change. The electronic states at the boundaries of allowed energy bands responsible for photostimulated

exoelectron emission were analyzed numerically, their structure being simulated with molecular orbitals and linear combination of atomic orbitals. The cluster models for this analysis were based on the most reliable data pertaining to the short-range order in the $PbO-SiO_2$ system (B.M.J. Smets, T.P.A. Lommen; JOURNAL OF NONCRYSTALLINE SOLIDS Vol 48 Nos 2-4, 1982; M. Imoka, H. Hasegawa, I.Yasui; JOURNAL OF NON-CRYSTALLINE Solids Vol 85 No 3, 1986). These models were tested for adequacy by comparing experimental and theoretical x-ray photoelectron spectra. Calculations were based on a discrete variation of x. The results of indicate that the $[Si_4O_4Pb](10+)$ cluster represents the structure of low-Pb glass ($x < 0.5$) and the $[Si_4O_4PbO_2 \times Si_2](14+)$ cluster, which contains both the SiO_4 tetrahedron and the PbO_3 pyramid, represents the hybrid skeleton of high-Pb glass ($x > 0.5$). Figures 4; references 13.

Duration of Signal in Meteoric Radio Channel

[Article by D.I. Kryukov and G.P. Davydov; UDC 523.53:621.396.946.1]

[Abstract] The average duration of meteoric radio echo at an image point while a meteoroid evaporates is calculated analytically by taking into account its dependence on the physical properties of a meteoroid and the trail with electron saturation concentration. First are determined the smallest meteoroid mass $m(0)$ detectable at some image point, the density of the atmosphere $\rho_{m(0)}$ within the meteoric zone, and the distance (normalized to height H of a homogeneous atmospheric layer) $x(0)= (h_{m(0)}-h_0/H$ from the altitude of maximum meteoroid ionization h_m to the altitude of an image point h_0. The system of equations for these three parameters is derived from the relation between lowest detectable electron concentration $n(0)= K_1 \times f(x(0)) \times m(0)$, the equation of classical theory $\rho_{m(0)}= K_2m(0)^{1/3}$, and the barometric relation $\rho_{m(0)}=\rho(0)exp[-x(0)]$. In the first approximation, for bright meteors, the function $f(x(0))$ is simulated with the Goerlofson distribution. A relation is subsequently established between the minimum detectable power and the minimum detectable electron concentration as the observation time decreases approaching the limit zero. From this relation is then obtained the duration t of an echo signal. Inasmuch as the mass m of an evaporating meteoroid is a random quantity with a probability density function of the $w(m)= cm^{-s}$ (c - constant, s - parameter), the average duration T of radio echo from such a meteoroid is calculated as the expectation value of the function of a random variable $T=$ Int $tm^{-s}dm$ from $m(0)$ to $m(\infty)$ divided by Int m^{-s} from $m(0)$ to $m(\infty) =$ $\tau[(s-1)/3 + \chi(m)^2/(3s-1)]$ (τ - time constant of meteoroid's trail, (gx(m) - one of the two possible values of χ in the relation $m(0)= [\rho(0)/K_2\chi(m)]^3$, only one of them being possible within the $\chi(m)= 0-3$ range). With accretions and fadings of an echo disregarded, an expression with s

within the 1.5-2.5 range is obtained for the duration T_0 of an echo at an image point. A meteoric radio channel with an isotropic distribution of radiants and an ellipsoidal scattering surface is considered for validating these analytical relations. The dependence of its average working cycle η [dash over η] on the length of its path L up to and beyond 1500 km has been evaluated on their basis and according to the $d^4\eta= td^4N$ relation (N - number of meteors, d^4 - fourth differential). With fadings also taken into account, there has also been evaluated the dependence of the average number of spikes N [dash over N] and of the average spike duration on the channel length. The average spike duration was found to be almost independent on the channel length, in close agreement with experimental data (H. Nes; IEEE PROCEEDINGS Vol 132 No 6, 1985), approximately equal to 0.4 s. Figures 2; references 8.

Feasibility of Amplifying Combination-Frequency Signals in Ionosphere Heated by High-Intensity Radio Emission

[Article by V.B. Avdeyev and A.P. Yarygin; UDC 550.388.2:621.731.166]

[Abstract] Increasing the amplitude A_Ω of Getmantsev-effect combination-frequency signals within the SLF to VLF range while heating the ionosphere with some intense radiation within the long-wave to short-wave region of the spectrum (PISMA V ZHURNAL EKSPERIMENTALNOY I TEORETICHESKOY FIZIKI Vol 20 No 4, 1974) is considered, namely by optimizing the parameters of that radiation. One possibility is generating many partial combination-frequency Ω-frequency signals with a cophasal polyharmonic spectrum and a Ω frequency separation between successive harmonics. Their superposition will yield a resultant combination-frequency signal whose amplitude can be increased by design without changing the total power of the heating radiation. As an example is considered a polyharmonic (M > 2) narrow-band ($f_M-f_1/f_1 << 1$ signal with an amplitude proportional to the sum of E_iE_{i+1} products from i= 1 to i= M-1, E_i denoting the amplitude of the electric field intensity of the i-th harmonic ($f_i= f_1 + (i-1)\Omega$) in the ionosphere. Two ways of attaining an amplitude E_i in the radiation spectrum of common long-wave/short-wave transmitters are analyzed and comparatively evaluated: double-sideband modulation and single-sideband modulation. The latter method is shown offer more possibilities of redistributing the total power over the radiation spectrum. It is noted that the amplitude A_Ω can decrease rather than increase when the signal has a noncophasal polyharmonic spectrum. Figures 1; tables 1; references 5.

Piezoelectric Pulse Interference Simulators

[Article by V.V. Nosov, candidate of technical sciences, and Yu.L. Spirin, candidate of technical sciences, Institute of Control Problems, Moscow; UDC 681.518.2]

[Abstract] Eighteen foreign-made piezoelectric interference simulators are recommended: 1) five (Schaffner NSG-222A/225, Noise Lab INS-410/420, ASEA-Haefely PB-4) for simulating exponential pulses of 50 ns duration with 5 ns rise time and 0-4000 V amplitude, 2) three (Schaffner NSG-504, ASEA-Haefely PU-12, Noise Lab LSS-712B) for simulating exponential pulses of 50 μs duration with 1.2 μs rise time and 500-5000 V amplitude, 3) two (Schaffner NSG-200E/224A) for simulating exponential pulses of 45 μs duration with 0.1 μs rise time and 0-2000 V amplitude, 4) three (Schaffner NSG-504, Noise Lab SWCS-932, ASEA-Haefely P3) for simulating segments of damped 1 MHz sine-wave segments with 200-3000 V amplitude of first half- wave, 5) five (Schaffner NSG-430/431, Noise Lab ESS-625/630, ASEA-Haefely PSD-15A) for simulating electrostatic-discharge pulses of 30 ns duration with 5 ns rise time from 150 pF capacitor banks. They all meet applicable IEC Standards, those in group 4 (NSG-505, SWCS-932, P3) also the IEEE 472 standard, and all except NSG-200E/224A also the CEMA 4702-84 Standard. Only experimental prototypes of Soviet-made simulators are available, built at the "Sigma" plant in Vilnius and at the "Elektronmash" plant in Leningrad. Two circuits with such a simulator are shown: 1) generator of linearly rising voltage with start-stop control triggering a master oscillator which feeds to a piezoelectric transformer signals of a frequency below resonance - transformer feeding signals through a rectifier diode to a high-voltage commutator switch - feedback from commutator output through detector and filter to stop button - blocking diode from transformer output to ground and bypass capacitor from rectifier output to ground; 2) controlled oscillator feeding voltage pulses to piezoelectric transformer carrying a row of N potential electrodes (connected to secondary voltage sources) for waveform regulation - transformer output pulse applied across load resistance - feedback from transformer output through filter to generator. The second circuit is designed primarily for controlling propagation of acoustic waves and movement of domain walls in the piezoelectric structure. Figures 2; tables 1; references 5.

Multilayer Printed-Circuit Boards With Compensating Layers

[Article by G.M. Khrobinskiy, candidate of technical sciences, Scientific-Industrial Association "Avangard", Leningrad; UDC 621.3.049.75:776.62- 555.621]

[Abstract] Design and fabrication of multilayer printed-circuit boards with compensating layers are analyzed, high precision and reliability requiring selection of a material with a coefficient of linear thermal expansion close to that of the material of mounted cases. The problem can be solved by deposition of an elastic coating or by reinforcement with interlayers of a fibrous material, kevlar or graphite fibers, having either a very small positive or a negative expansion coefficient. Another suitable material would be bilaterally copper-clad invar, but such a composite material is not produced in the USSR. A recommended solution is to include in the board metal expansion equalizing interlayers also serving as shields and high-conductivity paths for electric current supply or heat dissipation. Three variants of invar layers are proposed for rectangular size 170 x 200 mm^2= 340 cm^2 boards with 2-4 such interlayers: 1) 0.12 cm thick layers of grade 29NK-M-NT invar with a 167 cm^2 overall area, a few cutouts leaving an effective area equal to 64 percent of the 340 cm^2 board size; 2) 0.12 cm thick layers of grade 29NK-M-NT invar in the form of screens made of gage 2.5 mm wire, with a 167 cm^2 overall area and an effective area equal to 49 percent of the 340 cm^2 board size; 3) 0.1 cm thick layers of grade 42NAVI-NT invar with a 171 cm^2 overall area, many cutouts leaving an effective area equal to 50 percent of the 170 x 200 mm^2 board area. The nominal expansion coefficient of both invar materials is within the (4.5-5.5) x 10^{-6} 1/°C range. Such invar interlayers in boards with glass-textolite layers were tested in an environmental chamber. Their expansion coefficient was found to vary over the (4.5-8.0) x 10^{-6} 1/°C range (variant 1), (5.5-8.5) x 10^{-6} 1/°C range (variant 2), (6.0-9.0) x 10^{-6} 1/°C range (variant 3), and thus meet the requirements of All-Union State Standard 23752-79 for type-5 microcircuit cases. Invar interlayers (0.1 cm thick tape of grade 42NAVI-NT grade invar) were subsequently combined with 0.1 cm thick STF-1-35 glass-textolite layers, with 0.25 cm thick STF-2-35 glass-textolite layers, and with 0.06 cm thick STP-4 glass cloth. Such boards with two invar interlayers and bilaterally printed for mounting of electrical components were built and tested with such components (microcircuits, transistors, diodes, capacitors, resistors, transformers) for integrity of the electrical connections after cyclic fluctuations of the ambient temperature, after single and repetitive mechanical shock, after harmonic vibrations, and after fifty cycles of temperature change from -60°C to +120°C with 1 h holding time at each extreme point. Figures 4; tables 1; references 7.

Surface Wiring With Solder Pastes

[Article by S.N. Tyurin, engineer, I.A. Repina, engineer, V.N. Sirik, engineer, and A.M. Khabarin, engineer, Scientific-Industrial Association "Elektronpribor" (Electron Device), Yaroslavl; UDC 621.3.049.77.776: 621.3.035.21]

[Abstract] A technology has been developed for surface wiring of electronic components on ceramic (VK-94-1)

substrates with thick-film surface layers and on printed-circuit boards, the process involving use of solder paste: powder of solder alloy dispersed in organic binder. This paste (PPL-260) is thixotropic and its flash range is 180-230°C. It makes strong joints, also when leads and wires are not tinned. The paste must be thoroughly stirred before use. A board with thus soldered joints can be held for up to three hours, before the flux is wiped off after flashing in hot running water. An experimental study of the flashing process during surface wiring has revealed several advantages of ceramic board material over glass-textolite: better heat transfer and lower sensitivity to overheating with, consequently, less darkening. When wiring with this paste, flashing can be made to occur at temperatures up to 450°C within a down to 3 s heating time. Figures: 1; tables: 2.

Surface Wiring of Radio Components on Printed-Circuit Boards With Light Beam of Xe-Arc Lamp

[Article by N.A. Korobko, engineer, M.I. Oparin, candidate of technical sciences, N.S. Pronin, candidate of technical sciences, V.S. Mamayev, candidate of technical sciences, and V.A. Frolov, candidate of technical sciences, Moscow Institute of Aviation Technology; UDC 621.3.061.621.8.037]

[Abstract] The feasibility of wiring radio components on printed-circuit boards with radiation energy rather than by contact heating is considered on account of the obvious advantages. Most promising is shown to be use of a Xe-arc lamp, its radiation spectrum covering the 0.2-2.4 μm range of wavelengths and its efficiency being as high as 30-40 percent. It therefore is preferable to a 10.6 μm infrared CO_2-laser, because metals absorb shorter waves better than longer waves, and to an only about 1 percent efficient YAG:Nd^{3+} or other solid-state laser. Focusing the light with ellipsoidal reflectors is recommended for soldering. In an experiment with a 500 watt Xe-arc lamp, use of such optics made it possible to split the heating spot into to two equally large ones with a power density of 240 W/cm^2 on each and with their center-to-center distance variable over the 0-30 mm range. Throughout a soldering cycle the radio components did not heat above 70°C and the properties of the board material, SF-2 textolite, did not degrade. Figures 4.

Dipole Moments and Static Interaction of Ellipsoidal Particles in a Uniform Field

[Article by I. F. Binko, candidate of technical sciences, E. L. Nivenitsin (Kirov KVZRIU, Kiev),V. F. Reztsov, doctor of technical sciences (Institute of Electrodynamics, UkSSR Academy of Sciences, Kiev), A. L. Khadzhinov (Zaporozhtransformator Production Association, Zaporozhe); UDC 537.311.33]

[Abstract] Solution to the problem of electrostatic or magnetostatic interaction of ellipsoidal particles in a uniform field is used in many practical applications. While the value of the particle's charge (for electrostatic problems), or the value of the electric or magnetic dipole moments is generally assumed to be specified and independent of the particle's orientation with respect to the external magnetic or electric fields, in most cases a situation occurs when the macroscopic particles assume the dipole property only in the presence of the external field, and the magnitude and orientation of the dipole moments depend not only on the geometric dimensions of the particles, their electrophysical characteristics and other parameters, but on the particle's orientation with respect to the external field as well.

The particular features of the electrostatic interaction of ellipsoidal particles with the external uniform field and with each other were examined and expressions were obtained for induced dipole moments of these particles. Figures 2, references 7: 6 Russian, 1 Western.

Effect of Inductively Coupled Circuit on the Performance of the Excitation Winding With Cryogenic Resistance Operating in a Short-Duration Dynamic Mode

[Article by V. F. Bolyukh, candidate of technical sciences, V. G. Danko, doctor of technical sciences (KhPI); UDC 621.313:533.6.12:536.2.24]

[Abstract] With electromechanical pulse-operating devices, (electromagnetic mass accelerators, etc.) a considerably greater current density can be tolerated in current carrying elements, such as the excitation winding, compared to continuously operating devices because of a short duration of their working cycle. With these devices it may be advantageous to employ cryogenic resistance excitation winding, for example windings made of copper and cooled by cryogenic materials. Taking into account the electromagnetic and thermal processes the performance of a cryogenic excitation winding inductively coupled with the coil housing was examined operating in a dynamic mode under conditions when the heat exchange energy was greater than the
heat removed by the cryogenic cooling agent. The effects of dimensions, material, configuration of the metal chassis, and housing insulation of the inductor of a linear electrical motor on the nature of transient process in the cryogenic resistance excitation winding were established. Figures 5, references 12: 9 Russian, 3 Western.

Inducons Which Use Magnetic Conductors With Arbitrary Relationship of Geometric Dimensions

[Article by I. V. Volkov, corresponding member of the UkSSR Academy of Sciences, S. I. Zakrevskiy, I. I. Smolyanskiy, candidates of technical sciences (Electrodynamics Institute, Ukranian Academy of Sciences, Kiev), V. N. Sokolyanskiy (Institute of Pulsed Processes and Technology, Ukranian Academy of Sciences, Nikolayev); UDC 621.314.2]

[Abstract] The amount of metal and dimensions of the electrical equipment can be reduced with employment of inducons which are multifunctional hybrid elements. Because of their attractive features and increased application with the electrical equipment a further development is needed in the design methods and optimal construction of the inducons. A study was conducted to determine the feasibility of designing inducons made of magnetic conductors with geometrical dimensions which were selected for optimization of the electrical and thermal characteristics of these devices. Methods were developed for designing the fundamental parameters of the inducons. Figures 2, references 7 Russian.

Strategy Used in Developing a Generalized Structure of a Pulse Shaping Circuit for Control of a Direct Current Drive

[Article by O. N. Sinchuk, doctor of technical sciences, I. A. Lutsenko, candidate of technical sciences (KGRI, Krivoy Rog); UDC 622.002.5-83:658.26:621.31(075.8)]

[Abstract] Engineering characteristics of a DC drive with pulsed regulation are mainly determined by the architecture of the pulse shaping circuit (PSC) for the control system (CS)

The existing pulse shaping circuits which were previously developed based on the analog or digital technology, being sufficiently optimal for a particular application have a shortcoming in that they are not general enough. In this paper an attempt was made to develop the general principles for a structural realization of the PSC by a DC drive and to determine the limits of hardware and software application. A generalized mathematical model of the PSC was developed using the Petri theory and a synthesized structure of a hybrid two-phase

pulse shaping circuit proposed. The PSC structure was realized in practical application with an experimental system for controlling drives of industrial electric locomotives. Industrial tests of new samples supported the theoretical assumptions and conclusions. The PSC performs the following functions: control of a single-motor electric drive or independent control of a two-motor electric drive; 180° time shift in activation of the current interrupters; time-proportional or frequency-proportional control and automatic remote blocking of the controlling pulses. Figures 3, references 4 Russian.

Magnetic Interaction Between the Armature and Poles of a Shell-Type DC Electromagnet with Irregular Air-Gap

[Article by A. Ya. Kolchanov (Machine Science Institute, Ural Branch of Russian Academy of Sciences, Perm); UDC 621.335

[Abstract] Direct current shell electromagnets are used in electrical machine construction where these devices can be employed as weight compensators for an axial relief of the vertical rotor's support centers in electric motors, hydraulic-turbines etc. For a normal functioning of the compensator, the gap between the electromagnet's poles and the armature must be uniform. However, under some operating conditions an unbalanced electromagnetic force and the force moment are produced which have a perturbing effect on the rotors' dynamics. Methods were developed for computing the unbalanced electromagnetic force and its moment acting on the rotor taking into account the effect of the shell dc electromagnet with an irregular working gap on the rotor's dynamics. Figures 4.

Automated Dispatcher Control for a New Generation of Electrical Power Systems

[Article by V. N. Avramenko, V. A. Krylov, V. L. Prikhno, candidates of technical sciences (Electrodynamics Institute, Ukranian Academy of Sciences, Kiev); UDC [621.311:658.5.011.56](- 87)

[Abstract] The common electrical power system of the former Soviet Union is the world's largest centralized controlled energy association. A great number of computations related to the distribution of energy, control of energy level, activation or deactivation of power sources etc must be carried out in order to provide a reliable operation. These computations are so complex that they can be completed only with powerful computers. At the present time the electric energy systems of Ukraine, and the Commonwelth of Independent States use mainly third generation computers YeS-1020, YeS-1033, Yes-1036, YeS-1040, YeS-1045, YeS-1055, YeS-1061, whose power, as a rule, is not sufficient to assure the required degree of automation.

This review formulates the main features of the Automated Dispatcher Control of the new generation electrical power System (ADCS) and describes the structure of the integrated system for solution of electrical engineering problems of the dispatcher control. A short characteristic is provided of software elements for the new generation ASDC which was developed in the Ukranian Academy of Sciences Electrodynamics Institute. References: 9 Russian.

Local Parallel Construction of Graphs Whose Vertices Lie on a Plain

[Article by A. I. Adamatskiy, Petersburg State University; UDC 519.2]

[Abstract] Local parallel algorithms are described which are used for construction of certain graphs whose vertices are elements of a finite set of points on a plain. There are three types of graphs that can be constructed over a finite set of points on a plain: the Gabriel graph, the relative neighborhood graph, and the sphere of influence graph. These graphs are used in geographic variation analysis, plant ecology, data clustering and image recognition. The algorithms are designed for use with automatic cell processors. The non-synchronous determined non-stationary two-dimensional automatic cell devices where each cell is characterized by a variable size of the neighborhood graph constitute the mathematical model of the automatic cell processor. Figures 2; references 13: Russian 1, Western 12.

Architecture of Cyclic Parallel Computer Systems

[Article by S. C. Listrovoy, Krylov Military Engineering School for Rocket Forces, Kharkov; UDC 681.324:519.715]

[Abstract] Mathematical analysis of concepts governing the design of super-computers and other high-capacity systems is difficult because of their diversity, ill-defined concepts and absence of formalized research techniques. Problems related to organization of parallel computations and architecture of parallel computer systems are still not resolved. This paper examines different techniques used for designing problem oriented as well as universal parallel computer systems based on cyclic parallel computations. The following advantages were demonstrated. Employment of the cyclic computer systems makes it possible to reduce the equipment cost without loss of speed, because of fewer processors; the cyclic type systems can indefinitely increase their efficiency; these systems have no dead end situations due to simultaneous referral of processors to the same memory element, which causes the loss of efficiency of parallel computers with a common memory; with the cyclic parallel computers, high level programming languages can be developed in terms of conventional mathematical apparatus. Furthermore, it will be possible to design universal parallel computer systems based on cyclic computers, where the efficiency of the problem's solution will depend only on the quality of the algorithm structure.

It is pointed out that a conveyer type principle of computations appears to be most effective for organizing parallel computations. Since the development of the conveyer systems is now directed towards designing multiconveyers, the proposed concept of designing computer systems based on parallel cyclic computations constitutes an important step in the development of conveyer computers for super systems. Figures 11, references 7 Russian.

Model of High-Reliability Dispatcher of Parallel Computations

[Article by, V. N. Kustov, V. G. Burlov, Military Engineering and Space (study) Institute, St.Petersburg; UDC 681.324]

[Abstract] A method is described for reliable control of parallel computations using a simple dispatcher which functions on the bases of a previously prepared tabulated schedule in the multiprocessor computer system with a common memory. In this method a time redundancy was introduced for the purpose of increasing the reliability of parallel computations.

Solution of the dispatching problem consists of a sequential assignment of jobs following a specific plan as long as the probability of its execution P_{ex} is greater or equal to the specified admissible probability P_{ad}, and in the introduction of time redundancy in case P_{ex} is less than P_{ad}, so that the relationship P_{ex} greater or equal to P_{ad} would be fulfilled.

Statistical tests were carried out for evaluation of the dispatcher performance and the results are shown in the graphs. Figures 6, tables 3, references 5: Russian.

High-Speed Count Methods for Accessing Local Real-Time Computer Network

[Article by, A. Yu. Scheglov, Scientific-Technical Association Krasnaya Zarya, St. Petersburg; UDC 681.324]

[Abstract] High-speed methods are proposed for multiple access of distributed users of the real-time local computer network to a mono-channel. The method provides the value above 1 for the carrying capacity of the network communication channel under conditions of decentralized control of access and modular construction of the local computer network.

The proportional computer method for the local network subscribers access to the mainline consists in the following. Authorizations for the subscribers access to the

channel are transmitted by actual messages. Each sub-scriber is described by a current priority value. The subscribers identify the channel's occupation, as well as the moment when the channel becomes free. Then, assuming that all subscribers have received the access message, each message changes the current priority value of all subscribers by 1, but the authority for issuing a message after the channel becomes free is received by only one subscriber with a highest current priority. Other methods are described and the examples of their application are included.

It will be possible to construct failure-resistant small real-time local computer networks by employing the proposed count methods of access if the modular concepts which allow building-up the computer capacity are obeyed, and the control with parallel connection of subscribers to the channel is decentralized. Figures 2, tables 1, references 8: 7 Russian, 1 Western.

Field Topology and Physics of the Component Base of Bulk Integrated Microwave Circuits

[Article by V. I. Gvozdev, G. A. Kuzayev, Moscow Computer Design Institute; UDC 621.396.6]

[Abstract] Topology structures of electromagnetic fields were examined in new types of bulk integrated micro-wave circuits. Field lines behavior at critical points of the circuits was studied employing the topological approach to the electromagnetic field. Functional units in these circuits, which include phase shifter, power divider, directional coupler and filter were designed with improved electrical characteristics. Some particular dynamic features of the fields in the interconnectors were revealed.

Application of geometrical images to the electrodynamic theory makes it possible to describe the structure of the electromagnetic field and to construct its topology. The significance of the geometric approach lies in that new real horizons are being opened for understanding the complex electrodynamic phenomena.

Because of integration of the radio-electronic elements in the bulk of the microwave module it becomes necessary to treat the electromagnetic field as a three-dimensional object. The familiar circuit concepts can not yield a complete physical picture and help understand the bulk integrated circuit performance. The very philosophy of the layer-wise, planar and sequential signal processing is under scrutiny. The ideas of integral, three-dimensional approach to the signal processing are now becoming popular.

The following trends in the bulk integrated microwave circuit design are pointed out. It is possible to extend the topological method to the wave propagation and diffraction problem in three-dimensional waveguides. There are new prospects for application of the topological

approach to the reverse problems of electrodynamics. Figures 5, references 35: Russians 28, Western 7.

Reliability Analysis of Redundant LSIC Memory

[Article by P. P. Urbanovich, Minsk Radiotechnical Institute; UDC 681.3.07.62-192]

[Abstract] Methods were examined for predicting and estimating the probability and time before rejection, as well as the intensity of non-corrected rejections in redundant large scale integrated circuits (LSIC) memory, where codes are used for correcting single errors. Simplified engineering relationships which allow making reliability estimates with an acceptable accuracy were obtained. Computations demonstrate that a real improvement in the reliability of the redundant LSIC compared with the non-redundant depends on the length of coded words and lies within the limits of from 2 to 6-10 units. It was shown that for a relative memory area in a chip within 0.4-0.7, the time before rejection of a redundant LSIC with capacity of 16K can be increased by a factor of 1.5-4.0. Figures 3, tables 1, references 3: Russian 2, Western 1.

A Comparison of the Characteristics of Superconducting and Conventional Striplines in High-Speed Computers

[Article by R. A. Chentsov, A.A. Novikov, Institute of Precise Mechanics and Computer Technology of the USSR Academy of Sciences; UDC 538.945: 621.3.049.77:681.327]

[Abstract] At the present time feasibility of employing high temperature superconductivity (HTS) for computers draws considerable attention. In order to evaluate the advantages of superconducting striplines in semiconductor computers operating at cryogenic temperatures, computations were made of the characteristics of striplines made of high temperature superconducting materials and copper. Contemporary theory and experimental data on the conductors surface resistance as a function of frequency were used for the computations. A significant advantage was demonstrated of the superconducting lines over the lines made of conventional materials at frequencies above 1GHz.

In addition to new methods and computations a simple approach was developed for estimating the engineering parameters of superconducting materials. It is significant that the most recent published experimental data on physical properties of films made of high temperature superconducting materials were used for the computations.

When comparing the high temperature superconducting lines characteristics with the conventional one at a temperature of 77K it is worth mentioning that in the conventional materials the value of electroconductivity, which is the parameter that determines the signal distortion, is approaching its limits. On the other hand, as the technology advances, the parameters of the high temperature superconducting materials are being continuously improved. Further significant improvement of the HTS lines characteristic and increased probability of their application in computer technology can be expected with development of the HTS materials having a critical temperatures up to 100-125K. Figures 5, references 25: Russian 11, Western 14.

Controlling Capacity of Graded-Gap Charge Coupled Devices

927K0269D Moscow MIKROELEKTRONIKA
in Russian Vol 21, No 1, Jan 92 pp 58-62

[Article by V. M. Arutyunyan, S.G. Petrosyan, A. A. Karagezov, Yerevan State University; UDC 621.383.8: 621]

[Abstract] Some improvement of fundamental operating characteristics of charge coupled devices (CCD) were made by developing devices with a buried channel for charge transfer. Compared with the surface channel devices, the efficiency of charge transfer was improved and the mobility of the carriers in the channel was increased because of the effects related to their scattering at the boundary between semiconductor and dielectric. However, the shortcoming of these devices is a low controlling capacity. Since a greater controlling capacity is required for detecting the CCD output information with an acceptable signal to noise ratio, the feasibility of developing a buried channel using a graded-gap semiconductor structure for the charge coupled devices was examined in this paper.

It was demonstrated that with the graded-gap CCD it is feasible to significantly improve the controlling capacity compared to regular devices with a buried channel. Also, a feasibility exists in the graded-gap CCD of producing more favorable conditions for light conversion into a charge relief, both with a direct and reverse illumination. Figures 4, equations 9, references 9: Russians 5, Western 4.

Method for Integrating Mathematical Models of Electronic Circuits With Variable Increments

927K0254A Kiev ELEKTRONNOYE
MODELIROVANIYE in Russian Vol 14, No 1, Jan 92
pp 13-17

[Article by A. I. Tsifra, Kiev Polytechnical Institute; UDC 621.372.061.2]

[Abstract] A method for integrating mathematical models of electronic circuits was developed which makes it possible to increase the efficiency of the process of numerical integrations by employing the rarefaction property of the mathematical models.

The fundamental principle of the method lies in reduction of computation by using greater time increments for the mathematical model variables, which vary more slowly than others.

A theoretical and experimental study was conducted to determine the stability and convergence of the algorithm for integration of a non-linear algebraic differential system of equations with variable increments. The algorithm was tested for many practical problems involving the dynamic mode analysis of the electronic circuits.

It was pointed out in this paper that when developing the integration algorithm with variable increments one must be aware that the method can not be applied for the entire range of integration, and not for all electronic circuits. Therefore, a possibility of adapting this algorithm to the variation rate of the mathematical model variables must be considered. Figures 2, tables 2, references: 5 Russian.

Local Parallel Algorithm for Computation of the Voronoi Diagram

927K0254B Kiev ELEKTRONNOYE
MODELIROVANIYE in Russian Vol 14 No 1, Jan 92
pp 26-28

[Article by A. I. Adamatskiy, St. Petersburg State University; UDC 519.2]

[Abstract] Construction of the Voronoi diagram for a finite set of points on a plane is one of the most interesting problems of combinatorial geometry. Its solution consists of a construction of a polygon around every point p of a specified set, so that any point within this polygon lies closer to the point p than to any other point of the specified set. This problem can be applied in the fields of geography, crystallography, plant ecology, archeology and the image analysis. The most popular application of the Voronoi diagram is in problems dealing with a motion of robots through a limited two-dimensional area with obstacles.

In the applied problem which is examined in this paper it must be determined whether there exists a continuous trajectory of a collision-free motion of some solid body between two isolated sections of a limited two-dimensional region with a finite number of polygonal obstacles.

It was demonstrated that the Voronoi diagram, of a set of n points can be computed with an array of $O(n)$ processors in $O(1)$ beats. Figures 1, references 18: 1 Russian, 17 Western.

Synthesis of One-Dimensional Limited Systolic Computers of Two-Dimensional Discrete Fourier Transform

[Article by V. V. Kosyanchuk, N. A. Likhoded, P. I. Sobolevskiy, Institute of Mathematics of the Byelorus Academy of Sciences; UDC 681.3.012]

[Abstract] Studies related to hardware realization of two-dimensional discrete Fourier transform (2-DFT) using systolic structures have been intensified because of advances in the contemporary design technology of large scale integrated circuits and a practical requirement for a fast processing of the problem. The development of the LSIC computers imposes some limitations on the hardware volume and the number of input-output terminals, limitations which render the systolic computers projects with the number of processors linearly or quadratically dependent on the problem size unsuitable.

Because of this consideration the synthesis problem of one-dimensional limited systolic computers of the 2-DFT is of a current interest. The linear systolic computers are called one-dimensional if the input-output terminals are located only at the two last processor element, and they are called limited if they have a fixed number of processor elements which is independent of the problem size. In this paper two linear systolic computers of the discrete Fourier transform were synthesized. For this purpose two algorithms were examined. One consists of a product of three matrices, and the other

is based on the Gorner approach for computation of the elements of matrices. Figures 2, references 12: 7 Russian, 5 Western.

Logic Method for Analysis of the System Reliability Under Nonprobabilistic Estimates of the Elements Reliability

[Article by V. I. Levin, Penza, Institute; UDC 62-507:519.3]

[Abstract]The improbability theory of systems reliability is discussed in this paper where the elementary improbable quantities which characterize the system reliability constitute its base. The problem is to determine the relationship between these quantities.

The interval estimates of the moments of successive failure and recovery of elements of the entire system with determinate limits of these intervals were used in this paper as the elementary improbability quantities.

The obtained non-deterministic interval estimates of the system reliability being improbabilistic use a limited initial information on the elements reliability. These estimates are less informative than the probability estimates, however, it costs less to obtain, and therefore their application is justified. The improbabilistic estimates are useful when making a comparison between various types of the examined system structure during the design stages. References: 6 Russian.

Global Trends in the Development of Telecommunication

[Article by G. P. Zakharov, doctor of technical sciences, professor, department head of Leningrad Scientific Production Association "Krasnaya Zarya"]

[Abstract] Communication lines and Digital Concentrators of Packages (DCP) constitute the main facilities of the B-ISDN (Bus Integrated Service Digital Network). In turn, the productivity and the average delay time of the package are important requirements for the Digital Concentrator of Packages. The range of the DCP performance in terms of the required productivity is very wide. It varies from several thousand to several billions of packages per second. There are electronic and photon DCP. The electronic package commutators include commutators with a collective memory, collective medium and spacial separation. The photon package commutators have an electronic control or are fully optical. The productivity of the DCP with a collective memory is several thousand packages per second, the productivity of the DCP with a collective medium (bus) is much greater because of the parallel processing. However, the DCP with a spacial separation are more promising. A feasibility study was made in this paper of developing high efficiency DCP for the B.ISDN.

The N.ISDN-min are now employed in most countries without the necessity of making changes in the communication network. The B-ISDN are not yet universally implemented. Packaging of any kind of information, including high definition TV (HDTV) is not realizable at the present time. It appears that the idea of integrating the TV with other types of telecommunication must be rejected in favor of switching the cable TV programs by commutation of high speed channels.

When changing to the B.ISDN, a global approach is worth considering which will require a complete conversion of the network, but will produce a great economic effect. However, the draw back is, that initially there will not be enough subscribers with a 10Mbit/s interface. An effective approach of introducing the B.ISDN for the long-distance network may be in replacing the automatic exchange with the fast-acting DCP. Figures 4.

Ground-Based Stations With Small-Size Antenna

[Article by S. V. Borodich, Chief Scientist of the Scientific Research Radio Institute]

[Abstract]During the early stages of satellite communications, antennas with a "global coverage" were used which provided communication between continents. Because of the relatively small power of the satellite retransmitters, low-noise input amplifiers and high gain antennas were needed. Employment of such large ground-based stations with national systems is expensive. In order to be able to use less expensive ground stations, the radiation power from the satellite must be increased. This can be achieved by increasing the antenna gain using a narrow-beam antenna. The satellite communication is now possible with small ground-based stations VSAT (Very Small Aperture Terminal) stationed directly at the user location.

A network of small land-based receiving stations "Moskva" is operating in the Soviet Union. The antenna diameter is 2.5 m and the stations are operating in the 6 and 4 GHz frequency range.

Employment of the land-based stations with small size antenna for organization of satellite communication in rural areas would solve the telephone problems and contribute to the revival of villages and agriculture. Figures 1.

Organization of Telephone Time Service in Populated Places Located Within the Same Time Zone

[Article by Yu. A. Baranov, Scientist of the Moscow Communication Institute]

[Abstract] Because of the popularity of automatic time information service (Speaking Clocks) it must be expanded in the cities where it is available and organized in the telephone exchanges of other cities.

However, at the present time the development of the Speaking Clock service in most cities is held back by a limited availability of domestic equipment. Alternative technical solutions must be developed for providing this service to subscribers of the city exchanges that do not have the necessary equipment. Since in many regions of the country the inter-city channels are frequently not fully occupied, they can be used for transmitting one-way service information to the city exchanges located within the same time zone.

Practical measures for signal transmission from the Speaking Clock stations to the telephone exchanges of other cities are proposed in this paper and the described approach was implemented in cities of Odessa, Donetsk, and Poltava from the Speaking Clock equipment located in Kiev, and in the Gomel telephone exchange from Minsk, as well as in the Zhukovskiy exchange from Moscow. It was demonstrated that the system is reliable and useful for development of the Speaking Clock service in telephone exchanges located within the same time zone when the special equipment is not available. References 4: 3 Russian, 1 Western.

Mathematical Model for Selecting Induction Generators for Two-Machine Wind-Electric Power Sets

[Article by P.F. Vasko and P.P. Pekur, Kiev; UDC 621.311.24:621.313.332.0011.57]

[Abstract] Operation of a wind electric power plant with squirrel-cage induction generators driven by the windmill wheel through a speed reducer is considered, specifically a scheme with two such generators one behind the other coupled to the speed reducer output shaft: the main first generator with a higher nominal power P_1 followed by an auxiliary second generator with a lower nominal power P_2. A mathematical model is constructed as the basis for selection of both machines for such a set, the nominal power of the main generator determining the nominal power of the set. As the optimality criterion is regarded the normalized cost of such a set, namely its investment and depreciation cost plus operating cost. The operating cost, which is the cost of generating electric energy, depends not only on the performance characteristics of both induction machines and of the windmill wheel with speed reducer but also on the wind kinetics. The wind velocity, being a random function of time, is calculated according to a semiempirical formula based on a two-dimensional sequence of two random quantities: gust amplitude and gust duration. The normalized cost of operating such a wind electric power plant is minimized by imposing constraints on the nominal power and speed of the auxiliary generators: that not only $P_2 < P_1$ but also $n_2 < n_1$, n_1 (nominal speed of main generator) being determined by the aerodynamic characteristics of the windmill wheel as well as by the wind velocity, but also that P_2 of the auxiliary machine as induction motor (energized from a power line) be sufficient for accelerating the windmill wheel from standstill to nominal speed for adjustment or repair work during a period of calm air. There are then established both lower and upper limits of the range of wind velocity within which both generators will operate normally, also two conditions under either of which the main generator may be thrown into operation. The mathematical model thus contains nine equations of machine electromechanics and five operational constraints. An analysis of this scheme indicates that replacing a single induction generator with such a two-machine set will result in a 10-15 percent lower normalized cost of generating electricity with wind power. On the basis of this model have been selected a 250 kW - 1000 rpm main generator and a 45 kW - 600 rpm auxiliary generator with a single-output (one shaft) 20:1 speed reducer, each generator developing its nominal power at a wind velocity of 13.6 m/s, for 250 kW wind electric power plant to be installed in Crimea with windmill wheels 24 m in diameter carrying three vanes at a fixed angle and thus requiring automatic power regulation at higher than nominal wind velocities. Two sets of 250 kW - 1500 rpm and 45 kW - 750 rpm generators with a double-output (two shafts) 25:1 speed reducer have been selected for 500 kW wind electric power plants in Crimea with windmill wheels 31.5 m in diameter carrying three vanes at an angle appropriately variable at winds of higher than nominal velocities. Figures 1; references 11.

Experimental Determination of Current Flowing Through Human Body Under 220 V

[Article by A.Kh. Solobodkin and A.M. Stroganov; UDC 612.014.424:4:621.3.027.262.2.001.4]

[Abstract] Development of more effective safety measures for persons subject to electric shock in areas served by 220 V distribution networks is considered, it being necessary for this purpose to determine the current which will flow through the human body under such a voltage. This is done experimentally by controlled testing of people, a group of 66 persons having been selected for testing in two stages. In the first stage all 66 persons were tested with 100 V and the current under this voltage served as reference for estimating the current under 220 V by linear extrapolation, an empirical average magnification factor K= 20 accounting for the current rise due to nonlinearity of the voltage dependence of the body's impedance. In the second stage only 33 persons were tested with 220 V, the other persons having withdrawn because of pain or fear. The test apparatus for this experiment consists of an S8-13 "memory" oscillograph and a special synchronous commutator switch with special contactors. The test subject touches the electrodes with the palm of a hand at specified points and presses on them with increasing force till the cathode-ray tube of the oscillograph is automatically triggered once while voltage is applied to the electrodes through an electronic switch. When a sinusoidal alternating voltage is thus applied to the body, the instantaneous magnitudes and phases of the current flowing through it are measured on the oscillograms. The oscillograms also indicate the high-impedance range of a body under low voltage, the "hand-to-hand" loop current when both hands are involved, and the length of a body's reaction time. Oscillograms were, moreover, used for evaluating the dependence of the current amplitude on the active surface area of the electrodes and on the pressure on them. When a direct voltage is applied to the the body, tests with 180 V DC having been performed, the entire current transient is displayed on an oscillogram for measurement of both its "fast" and "slow" components. Statistical analysis of the test data yields the sought information in the form of histograms and the probability density functions, for men and for women. Typical results of 200-220 V tests reveal a characteristically wide variance of current levels not only in one and the same person but also from person to person, the current level depending largely on the amount of sweat and on the body's sensitivity during successive tests. According to the results of statistical analysis, the

expected current flowing through a body under 220 V AC is: in men 24.2 mA max (σ= 20.2) and 17.1 mA r.m.s. (σ= 14.3), in women 40.4 mA max (σ= 21.7) and 28.6 mA r.m.s. (σ= 15.3). Meanwhile, currents of 15-20 mA magnitude and 20 ms duration were found to cause pain and even involuntary jerking of hands. A standard Fourier analysis of oscillograms has revealed that the harmonic content of an alternating current in a body does not depend on its amplitude during the first voltage half-period and is evidently the same in all people. Considering that the current in a human body will climb above 100 mA within 100-130 ms, a protective disconnect device preset for activation by a current of 100 mA will not be adequate and the design of a more effective 220 V high-speed protective disconnect device must take into account 100-180 ms long reaction of the human body. Figures 7; tables 1; references 11.

Concluding Comments by Authors of Articles on Determination of Electromagnetic Forces in Magnetic Field

[Article by Ye.L. Lvov, doctor of technical sciences, Moscow Institute of Energetics; UDC 538.311.001.24]

[Abstract] Two articles on determination of electromagnetic forces in a magnetic field, one by Ye.L. Lvov (ELEKTRICHESTVO No 6, 1984) and one by A.V. Ivanov-Smolenskiy (ELEKTRICHESTVO No 7, 1985), have been followed by over 20 articles and comments (ELEKTRICHESTVO Nos 9,10,11, 1988; Nos 3,5,11, 1990) discussing the subject and related problems: 1) treatment of electromagnetic forces as the result of interaction of the magnetic field and molecular Ampere currents, according to Maxwell, in diamagnetic media as well as in paramagnetic and ferromagnetic ones; 2) equivalence, or rather nonequivalence, of Ampere's model to the physical field intensity and energy distribution; mutual independence of electric current and magnetic induction as condition for validity of Ampere's law; relation between intensity of microscopic field and macroscopic induction; torque of homopolar machine; 3) true volume and surface distributions of electromagnetic forces over a magnetized body; 4) hydrodynamic analogy, according to Maxwell, between magnetic effects; 5) magnetic field potential and, according to Maxwell, description of electromagnetic forces in terms of its gradient; 6) magnetostatic methods of determining electromagnetic forces; 7) set of independent criteria needed for satisfying the conditions of similitude; 8) theoretical and experimental data on deformation of magnetic flux carriers by electromagnetic forces. Altogether 14 articles in ELEKTRICHESTVO are cited (four by Ye.L. Lvov, four by A.V. Ivanov-Smolenskiy) in addition to four books: two by J.C. Maxwell, one by A. Einstein and I. Laub, one by I.Ye. Tamm. References 18.

Analytical-Numerical Method of Calculating Steady-State Temperature Field in Electromagnet with Forced Cooling

[Article by Yu.B. Antonov, Tomsk Polytechnic Institute; UDC 621.313.322-81:621.314:21.3.042.681]

[Abstract] For calculation of the steady-state temperature field in an electromagnetic with forced cooling, such an electromagnet is treated as a cylindrical structure consisting of heat radiators and passive elements. If the coolant transfers most of the generated heat to the ambient medium, then the axial heat flow is negligible in comparison with the radial heat flow. The internal heat sources are assumed to be known functions of the radial r-coordinate and the coolant is assumed to flow through channels in the streamline mode. Within each cooling channel (1) and within each radiator (2) is assumed to exist a coaxial cylindrical surface (radius $r_{1,2}$) gradient becomes zero and independent of the axial z-coordinate. The heat transfer from radiator to cooling channel is described by two partial differential equations of energy with appropriate boundary conditions including ambient temperature at one end face (z= 0). These two equations are supplemented with Lykov's formula for the rise above ambient temperature. The equation for a cooling channel is solved analytically with the aid of a finite Hankel integral transformation, assuming the thermal flux at the radiator-coolant interface to be known. The equation for a radiator, an Euler equation, is solved by letting $r= z_0 e^t$ and the heat loss in the winding be $q_w = \Sigma\, a_i r^{i-1}$ from i= 1 to i= N (i= 1,2,3,4 referring to iron core, winding insulation, copper conductors, and coolant respectively). The subsequent numerical solution proceeds in four steps: 1) determination of the two radii at which the temperature gradient is zero; 2) determination of the thermal flux at the radiator-coolant interface; 3) calculation of the temperature field $T_1(r,z)$ in a cooling channel according to Lykov's formula; 4) calculation of the temperature field $T_2(r,z)$ in the winding or, more precisely, the difference $T_2(r,z)$-$T_1(R,z)$ (R - radius of radiator and coolant interface). Owing to difficulties in calculation of the temperature field in a cooling channel according to Lykov's formula when $R < 1.2r_1$, it is in this case preferable to disregard the effect of surface curvature. Calculations made for a small betatron indicate that a 1 mm error in determination of r_1 leads to a not larger than 1°C error in determination of the maximum temperature. The results of calculations made for oil-cooled transformers agree closely with known experimental data. The author thanks V.S. Loginov, candidate of technical sciences and docent, for assistance in writing the article. Figures 1; tables 1; references 3.

Modernization of Ballistic Method for Measurement of Magnetic Flux

[Article by E.F. Kolotiy, I.P. Shelomov, and N.G. Mari-lov, Kramatorsk Industrial Institute; UDC 621.317.7]

[Abstract] Measurement of magnetic fluxes and induction with a ballistic galvanometer has several drawbacks, a major one being that the indicator needle moves while a reading is taken and its maximum deflection must be accurately marked. A second drawback is confinement of the instrument to a laboratory in a carefully set up permanent stand. A modern version of a ballistic instrument not only more reliable but also portable is, therefore, proposed for measuring magnetic fluxes of constant orientation. Its electric part includes a magnetizing coil and a measuring coil, an integrating operational amplifier with a voltmeter on its output side, and a DC power supply with a voltage regulator monitored by a voltmeter. The power supply energizes the magnetizing coil by sending a current to it through an ammeter and a switch, when the latter is closed. The measuring coil is loaded by a high resistance (1-5 kohm) across the input of operational amplifier. Use of a measuring coil with only a few turns will ensures that its internal resistance so much lower than the load resistance that almost its full output voltage will appear across the amplifier input. Use of an operational amplifier ensures ideal current amplification and consequently high accuracy of its output measurement. The operation of this instrument is explained on the basis of transient circuit analysis in accordance with Kirchhoff's second law. For measurement of small residual magnetic fluxes, reversing the direction of the magnetizing current by reversing the switch will double the flux reading and subtraction of half this reading from the previous one will yield the magnitude of the residual magnetic flux. If the time constant of the integrator (operational amplifier) can neither be determined by test nor accurately calculated, then the instrument must be graduated in units of magnetic flux. This done by determining two instrument constants, first its electric charge constant and then its magnetic flux constant. The determination of its electric charge constant can be made by any of the two known engineering methods, namely either with a standard mutual-inductance coil as reference or with a capacitor of known size. Figures 2; references 2.

Determination of Initial Reduced Dynamic Reluctance of Soft Magnetic Materials

[Article by V.V. Krokhin, All-Union Scientific Research Institute of Electrical Machines, Vladimir; UDC 621.318..1:538.24]

[Abstract] The reduced dynamic reluctance R of a soft magnetic material under dynamic conditions in a varying magnetic field and therefore being a function of the magnetic induction B is defined by the equation of state $dB/dt= R(B)[H(t)- H_s(B)]$, where H(t) denotes the magnetic field intensity at time t, H_s denotes the magnetic field intensity based on the static magnetization curve $B_s(H)$ which corresponds to the dynamic magnetization reversal curve with B= B(t), and R(B) denotes the reduced dynamic reluctance. One can refer R(B) to its initial value R(0) by letting R(B)= R(0)F(B), R(0) being the key parameter characterizing the dynamic behavior of any magnetic material and the dimensionless coefficient F(B) being a function of the magnetic induction which depends on the mechanism of magnetization reversal. Determining the magnitude of R(0) from that equation of dynamic state alone is difficult, because instantaneous values of four variables (B, dB/dt, H, H_s) must be known. It is proposed, therefore, to also use the energy loss per magnetization reversal cycle W= Int H(t)(dB/dt)dt from t= 0 to t= T with B(t)= B(max).f(ωt) (ω - reversal frequency). With the equation of dynamic state for dB/dt, this integral can be resolved into the sum of hysteresis loss and eddy-current loss. In the case of a sinusoidally varying magnetic induction there is then obtained an expression for the initial reduced dynamic reluctance as involving the reversal frequency, the initial magnetic permeability $\mu(0)$, and the both frequency-dependent and permeability-dependent loss tangent tanδ. The frequency dependence of tan$\delta/\mu(0)$ and of R(0) has been evaluated numerically for two magnetically soft ferrite materials 2000NM1 and 6000NM1. The results of calculations covering the 10-600 kHz range indicate that, while tan$\delta/\mu(0)$ increases monotonically at an increasing rate as the frequency of magnetization reversal is raised, R(0) first increases to maximum and then decreases. This trend is explained by the relation between the loss tangent and the magnetic characteristics of the material such as saturation magnetization, this relation being influenced by movement of domain walls and involving the mean distance between them. Figures 1; references 8.

Functional Characteristics of USSR Unified Power System

[Article by E.P. Volkov, V.A. Barinov, and A.S. Manev-ich; UDC 621.311.016.35.001.6]

[Abstract] Development of a 1150 kV electric power transmission network in the eastern zone of the USSR Unified Power System covering Siberia - Kazakhstan - Central Asia - Ural regions has been under consideration, this development to proceed in four stages and to be completed by the year 2010. Toward a validation of this project, the performance of such a network was analyzed for aperiodic static stability. Calculations were based on an equivalent circuit containing 221 nodes, 320 branches, and 67 generator plants with an 11,240 MW

total initial installed power and a 13,520 MW total installed power at the end of each stage. The capacity of Bratsk and Ust-Ilim hydroelectric power plants is to remain unchanged at 3040 MW and 3200 MW respectively, while the capacity of Krasnoyarsk and Sayano-Shushensk hydroelectric power plants is to be increased from present 2000 MW and 3000 MW to final 2900 MW and 4380 MW respectively. The results indicate that the capacity of Siberia - Kazakhstan sector can hardly be increased without radical restructurization of its basic network in the east-west direction. An important feature is the presence dominant underdamped low-frequency, 0.146 Hz and 0.217 Hz, modes. The results, together with the dynamic characteristics of Unified Power System networks already available, reveal that the static voltage characteristics of a load do not significantly influence the damping of these modes and that excitation regulators can be effective in damping these modes, but only excitation regulators with the appropriate transfer function. It is evident on the basis of this analysis and experience with power system unification in foreign countries that, from the standpoint of stability and viability, development of the USSR Unified Power System should proceed according to the principle of intraregional power and energy balance. Any departure from this principle will have to be convincingly justified on both technical and economic grounds. The role of interconnection ties between regions should remain to provide standby capacity, to maximize operating efficiency, and to optimize fuel economy. The same criteria will apply to development of a 1500 kV DC network in the eastern part of the USSR. Tables 3; references 7.

Method of Estimating Electrical Safety Level Under up to 1 kV Overhead Transmission Lines During Lightning Activity

[Article by M.Ye. Ierusalimov and Yu.Ya. Rybalchenko, Kiev; UDC 621.315.1:621.316.93:614.825.027. 26.001.24]

[Abstract] A method of quantitatively estimating the electrical safety level under overhead transmission lines during lightning activity is proposed, to facilitate optimizing the design of lightning protection for low-voltage (up to 1 kV) overhead transmission lines. The method is based on a probability forecast and uses as objective measure of electrical safety the probability of electrically incurred injury: $P_{el.inj} = P_{inc} P^*_{exc.en/inc}$ (P_{inc} - probability of a person being subject to an overvoltage at the instant of a lightning discharge, $P^*_{exc.E/inc}$ - conditional probability of excess energy above safe limit being released in person's body following one overvoltage incident). It takes into account indeterminacy of the struck target location and randomness of induced currents and voltages. The probability of a person being subject to an overvoltage at the instant of a lightning discharge is calculated according to the Erlang formula in queuing theory, assuming stationary Poisson distributions of

"person touching conductor" and consequent "overvoltage affecting person" events. The conditional probability of more than a safe amount of energy being released in a person subject to an overvoltage in one incident is calculated by including ij possible combinations of i-th of m zones of the overhead line within which a lightning may strike and j-th of q zones along the overhead line within which a person can stand at that time. Another factor included in the calculations is the probability of lightning currents affecting N persons simultaneously. The amplitude of an overvoltage wave is assumed to decay exponentially as it propagates from the struck target point: $V_s = V_0 \exp(-as^{1/2})$ (a - attenuation coefficient, s - distance traveled). Calculations by this method are demonstrated on 380 V transmission lines, such lines covering particularly large territories and supplying power to equipment constantly handled by humans. According to estimates based on numerical calculations by this method, the probability of a person inside a room with hookup to a 1 km long 380 V overhead line becoming injured by lightning is within the $(0.45\text{-}2.2) \times 10^{-7}$ in a territory subject to 50 hours of lightning activity in a year. Figures 1; tables 2; references 6.

Calculation of Inductance of Flat Busbars for Capacitive Energy Storage Cells

[Article by O.A. Antonyuk, A.M. Baltakhanov, and V.Ye. Bobikov, All-Union Scientific Research Center at All-Union Institute of Electrical Engineering imeni V.I. Lenin, Istra; UDC 621.316.35.001]

[Abstract] The inductance of flat busbars for capacitive energy storage cells is calculated by an integral method, in the approximation of ideal conductors and of a clearance between busbars much smaller than their characteristic linear dimension. The current is, moreover, assumed to enter and leave a busbar directly through its edges at a given density j in a plane-parallel magnetic field completely concentrated within the gap between busbars. Calculation of this magnetic field is reduced to solution of the first two-dimensional boundary-value problem for the scalar magnetic potential Ω within a region bounded by a contour $\delta^2\Omega/\delta\chi^2 + \delta^2\Omega/\delta\xi^2 = 0$ with the boundary condition $\Omega(s) = Int_s\, H_\tau ds = Int_s\, j_n ds$ (H_τ - tangential component of magnetic field intensity H, j_n - normal component of current density at busbar edge). This problem has first been solved analytically by the method of equivalent charges, involving superposition of all concentrated elementary currents whose resultant magnetic field will either be identical to or closely resemble the magnetic field of the busbars. It has then been solved numerically on a computer using the "KOLLEKTOR" program for flat busbars of arbitrary shape. Particularly interesting are: 1) solid trapezoidal busbars with the current entering only edgewise from the large base and both arms, then leaving only edgewise through the small base; 2) rectangular and triangular busbars with current entering only edgewise from all

sides, then leaving coaxially from the round edge of a center hole. An evaluation of these data indicates how the inductance of such busbars depends on the their shape and size. Figures 7; references 6.

Effect of Preliminary Electrification of Polyethylene on Length of Its Life in Pulsed Electric Field

[Article by O.S. Gefle and S.A. Lopatkin; UDC 621.315.616.9:621.317.333.8.001.6]

[Abstract] Considering that polyethylene is a nonhomo-geneous material consisting of a crystalline phase and an amorphous phase, buildup of electric charge at the interphase boundaries during preliminary electrification of this material is analyzed in terms of its effects on subsequent in-service life of this material. The analysis is based on the premise that buildup of electric charge can be effected by transfer of free carriers and by the gradient of relaxation polarization. Inasmuch as the relaxation polarization of dielectric polymers is determined not only by the orientation of dipole formations but also by the displacement of charge carriers within individual fragments of the supermolecular structure, the latter part of the relaxation polarization depends on both concentration and mobility of charge carriers as well as on the permeability of the interphase boundaries. Buildup of electric charge in turn causes a redistribution of the electric field within the specimen of dielectric material. Assuming an additive superposition of electric fields and considering that the intensity of the space-charge field is equal to the line integral of volume charge density minus the relaxation polarization, a method of regulating the electric field by regulating the buildup of volume charge is demonstrated on a plane-parallel specimen of low-density polyethylene. Then, on the basis of experimental data, is evaluated the effect of preliminary electrification of this material on the length of its life in a pulsed electric field of 75 kV/mm intensity. The results indicate that treatment with an electric field of 45 kV/mm intensity for 10 minutes will have the optimum effect: the charge concentrating sufficiently far from the surfaces of the electrodes (one grounded) to ensure negligible strengthening of the electric field inside the specimen and thus prevent breakdown, with the intensity of the space-charge field under the electrodes reaching 3-6 kV/mm. They also indicate that treatment of low-density polyethylene with a constant electric field will not produce a uniform charge distribution in a specimen and, therefore, not appreciably increase the volume charge density in it. In a pulsed external electric field superposed on the constant electrifying one, fewer pulses of opposite polarity than pulses of same polarity will increase the probability of breakdown (0.0-0.005-0.632-0.81). Modification of the surface by proton bombardment has been found to effectively weaken the electric field under the electrodes. Combining such a modification process with electrification can lengthen the life of low-density polyethylene appreciably under conditions favorable to low probability of breakdown, by a factor of 8.4 when the probability of breakdown is at the 0.05 level after both treatments of the material have been optimized. Figures 2; tables 2; references 8.

Selection of Economical Electric Power Supply for Rural Users Located Close to High-Voltage Electric Power Transmission Lines

[Article by A.A. Kasyanov, candidate of technical sciences, docent, and Khani Makhmud, engineer, "Labor's Red Banner" Belorussian Polytechnic Institute; UDC 621.316.001]

[Abstract] Considering that for rural users located far from urban electric power distribution networks but close to high-voltage electric power transmission lines it would be most economical to tap electric power directly from these lines, the problem of selecting the most economical type of substation is analyzed by the method of rub/kVA vs MVA and rub/kVA vs kW/km^2 diagrams. A substation is assumed to serve users within a circular territory, its radius and thus size being determined by the most economical radius of the distribution network. As criterion for selection from among the three available types of substation (transformer, inductive-reactor, capacitor) is chosen the total needed capital investment for each type. The results of a comparative numerical analysis covering all fixed and variable costs indicate that most economical for users far removed from 35 kV or 110 kV distribution lines will be a 220 kV transformer substation and that either a reactor substation or a capacitor substation will be more economical where the required voltage transformation ratio is smaller. Figures 3; tables 2; references 3.

Analog Part of Computer-Based Automatic Synchronizing Apparatus

[Article by F.A. Romanyuk, candidate of technical sciences, docent, F.A. Tishechkin, candidate of technical sciences, docent, and V.Yu. Rumyantsev, candidate of technical sciences, "Labor's Red Banner" Belorussian Polytechnic Institute; UDC 621.311:681.5]

[Abstract] Automatic synchronization of generators by means of a hybrid analog-digital apparatus is considered, the digital part including computer microprocessors and the analog part serving as a preparatory processor of the voltage data. Following the authors' previously proposed

version of an analog part containing mostly passive circuit components (IZVESTIYA VYSSHIKH UCHEB-NYKH ZAVEDENIY: ENERGETIKA No 4, 1991), an analog part built with operational amplifiers is now proposed. Before another generator is connected to an already operating system, this analog part of the synchronizing apparatus calculates its frequency by differentiating the monitored generator voltage and subsequently extracting average values of both its original and differentiated voltage. It then compares the thus determined generator frequency with the system frequency, for the digital computer logic to determine the instant of time when the switch is to be closed. The principle of this operation is based on the voltage phasor in accordance with theory of electrical machines. The structure of the analog part contains three input voltage step-down transformers, on their secondary side two operational amplifiers followed by an instrument voltage converter (full-wave rectifier with first-order low-pass smoothing filter) each and two resistive voltage dividers followed by an instrument voltage converter (full-wave rectifier with first-order low-pass smoothing filter) each, also an analog multiplexer followed by two operational amplifiers and each by an instrument converter (full-wave rectifier with second-order low-pass smoothing filter). All six voltage converters send their output signals to an integrating analog-to-digital converter (conversion time 60-80 ms). Binary signals are fed to a 16-digit microprocessor mounted on a single board. The microprocessor calculates, at a moderate speed of 10,000 oper/s, calculates within 0.5 s not only both generator and system frequencies but also the angle between the two generator voltage and system voltage vectors. The errors do not exceed 0.1-0.15 Hz and 1-2° respectively. Such a scheme ensures a high interference immunity of automatic synchronization and that all necessary information is provided in time for switch closing. Figures 2; references 3.

Regulator for Diagnostic Insulation Testing Apparatus

[Article by V.M. Prikhodko, candidate of technical sciences, docent, "Labor's Red Banner" Leningrad Institute of Water Transportation; UDC 621.315.2.048: 621.3.072.2:621.3.032]

[Abstract] A portable electronic 0-380 V voltage regulator has been developed for the diagnostic insulation testing apparatus used in the Central Electric Network under the Far Eastern Regional Administration of Power System Management, specifically for testing insulation of 6-10 kV overhead transmission lines with rectified voltage and for locating insulation defects along these lines. Its active components are four silicon diodes, two power diodes, three MP25 transistors, one thyristor, two power thyristors, and three stabilitrons. The power diodes and thyristors are of class-9 or better with respect

to repetitive peak reverse voltage. The passive components include 15 resistors from 5 Ω to 22 kΩ, one shunt with 75 mV and 300 A rating, one 1 μF - 250 V capacitor, two 4 μF - 600 V capacitors, and a switch. The regulator is reliable and highly efficient, also noiseless. It ensures smooth regulation of the arc-over current and is suitable for remote control. Its power rating is 30 kVA maximum and its current capacity is 150 A maximum. It will generate strong high current harmonics when current is sent through a high-voltage line from an ETL-35 electrical testing laboratory. The regulator occupies a small space, weighs 20 kg, and is fireproof. Using it is the Central Electric Network should save 10,000 rubles annually. Figures 2; references 4.

Problems Involved in Raising Effectiveness of Moscow Power System Operation in Transition to Market Economy

[Article by Ye.K. Kuznetsov, Moscow Regional Administration of Power System Management; UDC 621.31.338.4]

[Abstract] Transition of the Moscow Power System to a market economy and attendant problems in raising the effectiveness of its operation are examined, as guide serving the experience of the past 30 years and forecasts projecting to the year 2010. Attention is focused on the necessity of adjusting the budget so as to adequately cope with the avalanche mode of equipment aging and with physical wear of equipment detrimentally affecting its reliability economy, with related power failures and required shutdowns. Into account must be taken cost of renovation and development as well as the inflationary rise of fuel and labor costs. This calls for a revisions of the rate structure as well as of the load and demand curves for the sake of balancing the budget. How these aspects of transition affect the Moscow Power System is demonstrated on its heat and electric power plants. An analysis of available relevant data indicates that better fuel economy will play the decisive role here, another important factor being selection of the best strategy for equipment development and installation. Such a strategy may include design of new small gas turbine plants for small towns. It should also involve conversion of the military industry to commercial status and thus and thus ensure quick organization of series production of needed new equipment. Figures 7; tables 1.

Test Circuits and Equipment in Mobile High-Voltage Laboratories

[Article by P.I. Afonskiy, engineer, and G.N. Pyatachenko, engineer, Donets Basin Regional Administration of Power System Management; UDC 621.317.2]

[Abstract] The two mobile high-voltage laboratories now built at the Yaroslavl Electromechanical Equipment Manufacturing Plant for the USSR Ministry of Energy are the ETL-35-02 M based on the model GAZ-66 vehicle and the ETL-10-02 based on the model GAZ-52 vehicle, both vehicles being built at the Gorkiy Automobile Manufacturing Plant. The ETL-35-02 M laboratory is designed for startup-tuneup and preventive testing of 35 kV and higher-voltage equipment, but it lacks facilities for measuring the short-circuit impedance of power transformers, for measuring the resistances of 110 kV and higher-voltage transformer windings by the ammeter-voltmeter method with a direct current of even as low as 5-10 A, for measuring the contact resistances in air and oil circuit breakers, for measuring the tan σ and thus the tan δ of bushings on high-power transformers by the standard method, and for matching the 100/20 V - 20 kVA test transformer to the about 8 kVA regulator. The ETL-10-02 is not even a laboratory in the strict sense, its 12 kW generator with the set of instruments for startup-tuneup and preventive testing of 6-10 kV substation equipment and overhead transmission lines not conforming to latest safety rules. Both laboratories, moreover, have no apparatus for locating faults in 6-10 kV cables by the arc-over method. It is recommended, therefore, that the ETL-10-02 be withdrawn from production and the ETL-35-02 be modified so as to incorporate all these missing features. As a crude model may serve the mobile high-voltage laboratory used by the Krasnoluchsk group operating the electrical networks under the Donets Basin Regional Administration of Power System Management. This mobile laboratory includes all the required instrumentation and circuitry. It can be further enhanced by development and addition of a switch for tapping the high-voltage winding of the arc-over transformer under voltage, a set of devices already developed at the Novocherkassk Polytechnic Institute for locating single-phase faults in cables, and a needle-indicator instrument such as the German-made for determining the cable burial depth. Figures 1.

New Developments in Soviet Cable Technology

*927K0172A Moscow ELEKTROTEKHNIKA in Russian
No 11, Nov 91 pp 4-7*

[Article by I.B. Peshkov, doctor of technical sciences, presiding administrative officer, All-Union Management Association "Elektrokabel" (Electric Cable); UDC 621.315.2/3.001.8

[Abstract] Noteworthy latest developments in Soviet high-voltage cable technology are: high-strength (8 kV/ mm) minimum-thickness insulation system formed by deposition of a radiating high-permittivity ($\varepsilon \approx 4.5$) coat on the metal shield, deposition of three layers (radiative - conducting - insulating) in one pass, and subsequent vulcanization under pressure in a dry inert gaseous atmosphere or in a liquid coolant; polyethylene tape modified with dicumyl peroxide, vulcanized in a nitrogen atmosphere by gradiental heating to 180°C and subsequent compression under up to 2.5 MPa, for winding as insulation material around cable potheads and sleeve joints filled with a fluid organosilicon compound or around cable leads to transformers and other SF_6-filled apparatus; bombardment of polymer materials with a fast-electron beam for increasing their heat resistance and, upon addition of special agent, also their radiation resistance so that the allowable operating temperatures can be raised from 70-80°C to 120-150°C and the overall cable diameter can be reduced by 20-40 percent; conversion of some thermoplastic materials into thermosetting ones such as polyvinyl chloride by means of modifiers without irradiation; special winding machine with remote control to replace multipass rolls for better continuity and higher power efficiency, also special systems of electron-beam control; new technique of laying corrugated screen wires longitudinally on a cable core, and use of perforated copper ribbons as outer conductors of radiating radio-frequency cables. Figures 4; tables 1.

Model EAM1 Self-Contained Electric AC Servo Drive

*927K0172B Moscow ELEKTROTEKHNIKA in Russian
No 11, Nov 91 pp 13-16*

[Article by V.M. Nikitin, candidate of technical sciences, D.A. Pozdeyev, candidate of technical sciences, A.A. Prokudin, engineer, and V.M. Pimenov, engineer; UDC 62-83:621.313.3.001.8]

[Abstract] A self-contained multicoordinate electric AC servo drive with microprocessor control and a set of up to six motors covering the 0.23-17 N.m torque range has been developed, this EAM1 servo drive featuring independent control of each motor and thus of the motion along any of up to six coordinates. The power supply, a 3-phase full-wave 300 V rectifier with a capacitive filter and a transistor switch, draws power from the 220 V line through a matching power transformer and includes a rheostat for braking. Each regulator is a transistor current inverter connected across the 3-phase motor

winding. Each motor can run in seven modes: 1) pull-back to zero coordinate defined in terms of physical position or by control program; 2) pull-in to given constant speed with given limits on acceleration; 3) single travel through given distance, precisely within one discretization step of optical pulse-type displacement transducer; 4) positioning in accordance with user's program; 5) execution of programmed logic operations pertaining to control of driven object; 6) transition from one constant speed to another in accordance with composite tachogram without stoppage of the driven object; 7) tracking by responding to discrete signals with displacement information arriving from upper-level computer or special numeric program control system at a repetition rate not higher than 500 Hz. Each motor can be tested in running modes either unrelated or related to motion of the driven object. Each motor can continue running in accordance with a given program after having been disconnected from the indicators and controls panel, to allow programming other motors, and then after having been reconnected. When running in any mode, the drive can be stopped and restarted either by manual control with by push buttons disconnecting and reconnecting it to the power supply or by automatic control with electrical logic through 11 inputs (0 - emergency shutdown, 1 - terminal switch, 2 - terminal zero-position switch, 3 - stop, 4 - start, 5 - response, 6 - external condition 1, 7 - external condition 2, 8,9,10 - select any of seven programs) and 8 outputs per motor (coordinate). The drive can be produced on a commercial scale and offers several advantages in the design of numeric program systems for multicoordinate drives, one of them being that it is compatible with any personal computer (DVK, Standard System 1840, IBM) through an interfacing 9600 baud IRPS radial channel or an MPK multiplexed sequential channel. Figures 3; tables 2.

New Generation of Micaceous Electrical Insulation Materials for Low-Voltage Apparatus

*927K0172C Moscow ELEKTROTEKHNIKA in Russian
No 11, Nov 91 pp 16-19*

[Article by V.V. Rozhkov, candidate of chemical sciences, M.L. Pustylnik, candidate of chemical sciences, A.I. Lebedev, candidate of chemical sciences, and L.P. Tkacheva, engineer; UDC 621.315.613:621.313]

[Abstract] While micaceous papers for class F and class H heat- resistant electrical insulation are being produced in the USSR, mica-fiber paper made of muscovite and mica-plastic paper made of phlogopite, new grades of micaceous insulation are being now introduced in two forms: tape and sheet. The tape grades for DC and AC windings are: LSAS-10 (min 30 wt. percent mica, class F, thickness 0.08-0.15 mm, dielectric strength 30 kV/mm), LIKO-TT (min 35 wt. percent mica, class H, thickness 0.15-0.21 mm, dielectric strength 14 kV/mm), LSETF-PM (min 23 wt. percent mica, class H, thickness 0.16-0.19 mm, dielectric strength 35 kV/mm). The sheet grades for commutators and slip rings are: KIFE (max

7.5 wt. percent binder, thickness 0.40-0.80 mm, dielectric strength 22 kV/mm) and KIFE-A (max 9.0 wt. percent binder, thickness 0.80-1.5 mm, dielectric strength 22 kV/mm) with EP-9158 epoxy resin + BF_3 hardener as binder, FIFK-T (82-90 wt. percent mica, thickness 0.25-0.50 mm, dielectric strength 36 kV/mm average and 24 kV/mm minimum) with modified organosilicon compound as binder. Tables 6; references 3.

New Ways of Utilizing Information Technology in Power Supply Systems

927K0172D Moscow ELEKTROTEKHNIKA in Russian No 11, Nov 91 pp 35-37

[Article by B. Haries, doctor of engineering, Koeln (Germany)]

[Abstract] With information technology playing an important role in remote control of power generation and distribution, the trend since the late nineteen seventies has been toward use of optical communication systems for this purpose. Such systems include infrared laser diodes as sources of light (850 nm, 1300 nm, 1550 nm) and optical fibers in cables as conductors for data transmission. Either graded-index or single-mode fibers are used, bundles of them laid inside small tubular steel sheaths. A system with underwater fiber-optic cables has already in 1984 been installed along the Baltic coast of Germany serving two platforms for off-shore oil drilling operations (information signals transmitted at rate of 19.2 kbit/s, low-frequency signals transmitted at rate of 64 kbit/s, 850 nm light used for covering distances up to 20+ km, 1300 nm light used for covering distances up to 40+ km). Optical communication systems are now used not only for measurement, control, and regulation, but also for long-distance differential or other protective relaying. An example is the fiber-optic lightning protective cable built by the Felten & Guilleame Company in 1988. These cables run along high-voltage lines, the latest trend being to build them into electrical power cables, stranded flexible conductors, and overhead lines. Figures 2; tables 2.

St.Petersburg State Technical University and "ELVO" Scientific-Industrial Association

927K0172E Moscow ELEKTROTEKHNIKA in Russian No 11, Nov 91 p 45

[Abstract] Three type UKhL1 support hoops for 50 Hz and 60 Hz high-voltage transmission towers have been developed jointly by the St.Peterburg State Technical University and the "ELVO" Scientific-Industrial Association: ShOS-330B-1-UKhL1 for 330 kV towers, ShOS-500B-1-UKhL1 for 500 kV towers, ShOS-750B-1-UKhL1 for 750 kV towers. All three are designed for installation at up to 1000 m altitudes above sea level, for operation at ambient temperatures from -60°C to +40°C, and to withstand wind velocities not higher than 40 m/s. Each consists of a base insulator, a set of shields, and a bracket. The base insulator is a colonnade of thin glass-plastic rods coated with a tracking-resistant compound. An insulator made of this composite material does not break during seismic activity under a substation. It requires 3-5 times less material and can be about 25 percent shorter than one made of porcelain. It also requires fewer shutdowns for cleaning or replacement. The design of these support hoops are original, no similar ones existing anywhere in the world, and is covered by eight patents. Figures 3; tables 1.

This is a U.S. Government publication. Its contents in no way represent the policies, views, or attitudes of the U.S. Government. Users of this publication may cite FBIS or JPRS provided they do so in a manner clearly identifying them as the secondary source.

Foreign Broadcast Information Service (FBIS) and Joint Publications Research Service (JPRS) publications contain political, military, economic, environmental, and sociological news, commentary, and other information, as well as scientific and technical data and reports. All information has been obtained from foreign radio and television broadcasts, news agency transmissions, newspapers, books, and periodicals. Items generally are processed from the first or best available sources. It should not be inferred that they have been disseminated only in the medium, in the language, or to the area indicated. Items from foreign language sources are translated; those from English-language sources are transcribed. Except for excluding certain diacritics, FBIS renders personal names and place-names in accordance with the romanization systems approved for U.S. Government publications by the U.S. Board of Geographic Names.

Headlines, editorial reports, and material enclosed in brackets [ ] are supplied by FBIS/JPRS. Processing indicators such as [Text] or [Excerpts] in the first line of each item indicate how the information was processed from the original. Unfamiliar names rendered phonetically are enclosed in parentheses. Words or names preceded by a question mark and enclosed in parentheses were not clear from the original source but have been supplied as appropriate to the context. Other unattributed parenthetical notes within the body of an item originate with the source. Times within items are as given by the source. Passages in boldface or italics are as published.

SUBSCRIPTION/PROCUREMENT INFORMATION

The FBIS DAILY REPORT contains current news and information and is published Monday through Friday in eight volumes: China, East Europe, Central Eurasia, East Asia, Near East & South Asia, Sub-Saharan Africa, Latin America, and West Europe. Supplements to the DAILY REPORTs may also be available periodically and will be distributed to regular DAILY REPORT subscribers. JPRS publications, which include approximately 50 regional, worldwide, and topical reports, generally contain less time-sensitive information and are published periodically.

Current DAILY REPORTs and JPRS publications are listed in *Government Reports Announcements* issued semimonthly by the National Technical Information Service (NTIS), 5285 Port Royal Road, Springfield, Virginia 22161 and the *Monthly Catalog of U.S. Government Publications* issued by the Superintendent of Documents, U.S. Government Printing Office, Washington, D.C. 20402.

The public may subscribe to either hardcover or microfiche versions of the DAILY REPORTs and JPRS publications through NTIS at the above address or by calling (703) 487-4630. Subscription rates will be provided by NTIS upon request. Subscriptions are available outside the United States from NTIS or appointed foreign dealers. New subscribers should expect a 30-day delay in receipt of the first issue.

U.S. Government offices may obtain subscriptions to the DAILY REPORTs or JPRS publications (hardcover or microfiche) at no charge through their sponsoring organizations. For additional information or assistance, call FBIS, (202) 338-6735,or write to P.O. Box 2604, Washington, D.C. 20013. Department of Defense consumers are required to submit requests through appropriate command validation channels to DIA, RTS-2C, Washington, D.C. 20301. (Telephone: (202) 373-3771, Autovon: 243-3771.)

Back issues or single copies of the DAILY REPORTs and JPRS publications are not available. Both the DAILY REPORTs and the JPRS publications are on file for public reference at the Library of Congress and at many Federal Depository Libraries. Reference copies may also be seen at many public and university libraries throughout the United States.